Acta Cryst E CRYSTALLOGRAPHIC COMMUNICATIONS

ISSN 2056-9890

Crystal structure, Hirshfeld surface and energy framework analysis of bis{3-(benzofuran-6-yl)-5-[6-(1*H*-pyrazol-1-yl)pyridin-2-yl]-1*H*-1,2,4-triazol-1-ido}iron(II) methanol disolvate

Illia Terpeliuk,[a] Kateryna Znovjyak,[a] Sergiu Shova,[b] Olexandr V. Oksiuta,[c] Vladimir M. Amirkhanov,[a] Igor O. Fritsky[a] and Maksym Seredyuk[a]*

[a]Department of Chemistry, Taras Shevchenko National University of Kyiv, Volodymyrska Street 64, Kyiv, 01601, Ukraine, [b]Department of Inorganic Polymers, "Petru Poni" Institute of Macromolecular, Chemistry, Romanian Academy of Science, Aleea Grigore Ghica Voda 41-A, Iasi, 700487, Romania, and [c]Institute of Organic Chemistry, National Academy of Sciences of Ukraine, 5 Academik Kukhar Street, 02094, Kyiv, Ukraine. *Correspondence e-mail: mlseredyuk@gmail.com

Received 20 August 2025
Accepted 2 October 2025

Edited by A. Briceno, Venezuelan Institute of Scientific Research, Venezuela

Keywords: crystal structure; iron(II) complexes; neutral complexes; tridentate ligands.

CCDC reference: 2492851

Supporting information: this article has supporting information at journals.iucr.org/e

The title compound, $[Fe(C_{18}H_{11}N_6O)_2]\cdot 2CH_3OH$, crystallizes in the orthorhombic space group *Pbcn* (No. 60) with half of the complex molecule and a methanol molecule in the asymmetric unit. In the complex, the two tridentate 3-(benzofuran-6-yl)-5-[6-(1*H*-pyrazol-1-yl)pyridin-2-yl]-4*H*-1,2,4-triazol ligands meridionally bind to the central Fe^{II} ion through the N atoms of the heterocyclic groups, forming a pseudo-octahedral coordination sphere. In the crystal, C—H(pz)···π(ph) and C—H···N/C/O interactions consolidate the structure. Energy framework analysis at the B3LYP/6–31 G(d,p) theory level was performed to quantify the interaction energies in the crystal.

1. Chemical context

3*d*-Metal complexes featuring tridentate bisazolepyridine ligands constitute a versatile class of coordination compounds with applications in biochemistry (Fares *et al.* 2020), catalysis (Wei *et al.*, 2015) and molecular magnetism (Halcrow 2024). For ligands with asymmetric architectures, where one azole moiety bears a protonated nitrogen heteroatom, deprotonation can balance the charge of the central metal ion, yielding neutral complexes. In this case, the peripheral substituents on the neutral complexes influence intermolecular interactions, which in turn affect the connectivity, binding energy, crystal packing, and the coordination environment of the central ion.

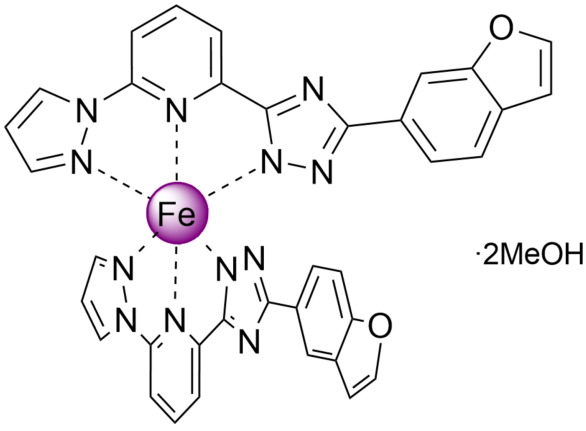

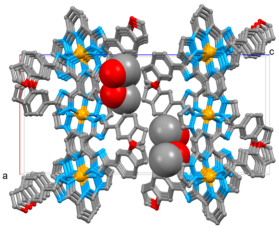

Given the prominence of bisazolepyridines as ligands in the Fe^{II} spin-crossover domain, and motivated by our long-

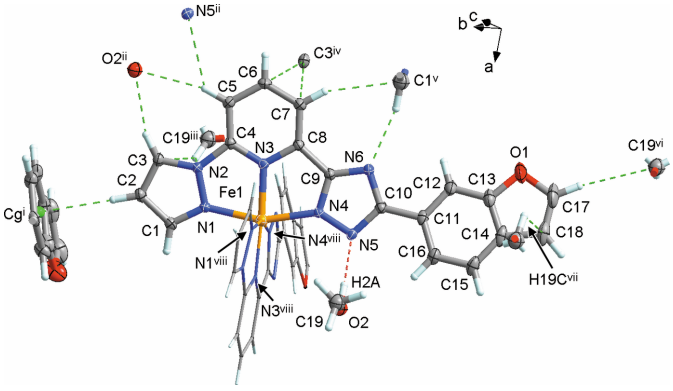

Figure 1
The molecular structure in the asymmetric unit of the title compound and contact atoms with displacement ellipsoids drawn at the 40% probability level. The second ligand is shown in wireframe style for clarity. The strong O—H···N (red) and weak C—H···N/C/O/π (green) hydrogen bonds are shown with the nearest neighbours. Symmetry codes: (i) $1-x, 1+y, \frac{1}{2}-z$; (ii) $\frac{1}{2}+x, \frac{1}{2}+y, \frac{1}{2}-z$; (iii) $1-x, y, \frac{1}{2}-z$; (iv) $\frac{3}{2}-x, -\frac{1}{2}+y, z$; (v) $\frac{1}{2}+x, -\frac{1}{2}+y, \frac{1}{2}-z$; (vi) $\frac{1}{2}+x, \frac{1}{2}-y, 1-z$; (vii) $1-x, 1-y, 1-z$; (viii) $1-x, y, \frac{1}{2}-z$.

standing interest in complexes of 3*d*-metals with N-heterocyclic ligands (Seredyuk *et al.*, 2007; Bonhommeau *et al.*, 2012; Piñeiro-López *et al.*, 2018), herein we report a new neutral low-spin complex based on the asymmetric ligand 3-(benzofuran-6-yl)-5-[6-(1*H*-pyrazol-1-yl)pyridin-2-yl]-4*H*-1,2,4-triazol. This study details the synthesis and crystal structure of the title compound, incorporating benzofuran groups to tune intermolecular interactions.

Table 1
Hydrogen-bond and short contact geometry (Å, °).

D—H···A	D—H	H···A	D···A	D—H···A
O2—H2A···N5	0.85 (3)	1.89 (2)	2.750 (2)	178 (3)
C1—H1···N6^{i}	0.95	2.27	3.189 (2)	163
C3—H3···O2^{ii}	0.95	2.29	3.208 (2)	161
C5—H5···O2^{ii}	0.95	2.46	3.386 (2)	164
C5—H5···N5^{ii}	0.95	1.90	3.463 (2)	129
C7—H7···C1^{iii}	0.95	2.63	3.537 (2)	159
C19—H19A···N2^{iv}	0.97	2.74	3.491 (2)	133
C19—H19A···C3^{iv}	0.97	2.89	3.695 (2)	140
C6···C3^{v}	–	–	3.482 (2)	–
C7···C3^{v}	–	–	3.498 (2)	–

Symmetry codes: (i) $x-\frac{1}{2}, y+\frac{1}{2}, -z+\frac{1}{2}$; (ii) $x+\frac{1}{2}, y+\frac{1}{2}, -z+\frac{1}{2}$; (iii) $x+\frac{1}{2}, y-\frac{1}{2}, -z+\frac{1}{2}$; (iv) $-x+1, y, -z+\frac{1}{2}$; (v) $-x+\frac{3}{2}, y-\frac{1}{2}, z$.

2. Structural commentary

The title compound, $[Fe(C_{18}H_{11}N_6O)_2]\cdot 2CH_3OH$, crystallizes in the orthorhombic space group *Pbcn* (No. 60) with half of the complex molecule and a methanol molecule in the asymmetric unit. In the complex, the two ligands meridionally bind to the central Fe^{II} ion, which lies on a twofold rotation axis through the N atoms of the heterocyclic groups, forming a pseudo-octahedral coordination sphere. The benzofuran group of the ligand is rotated by 16.2 (2)° relative to the almost planar pyrazole-pyridine-triazole (pz-py-trz) fragment (r.m.s. deviation = 0.055 Å). The methanol molecule forms hydrogen bonds with the trz rings (Fig. 1). The central Fe ion has a distorted octahedral N_6 coordination environment formed by the nitrogen donor atoms of the tridentate ligands. The average bond length iron–nitrogen (<Fe—N>) of

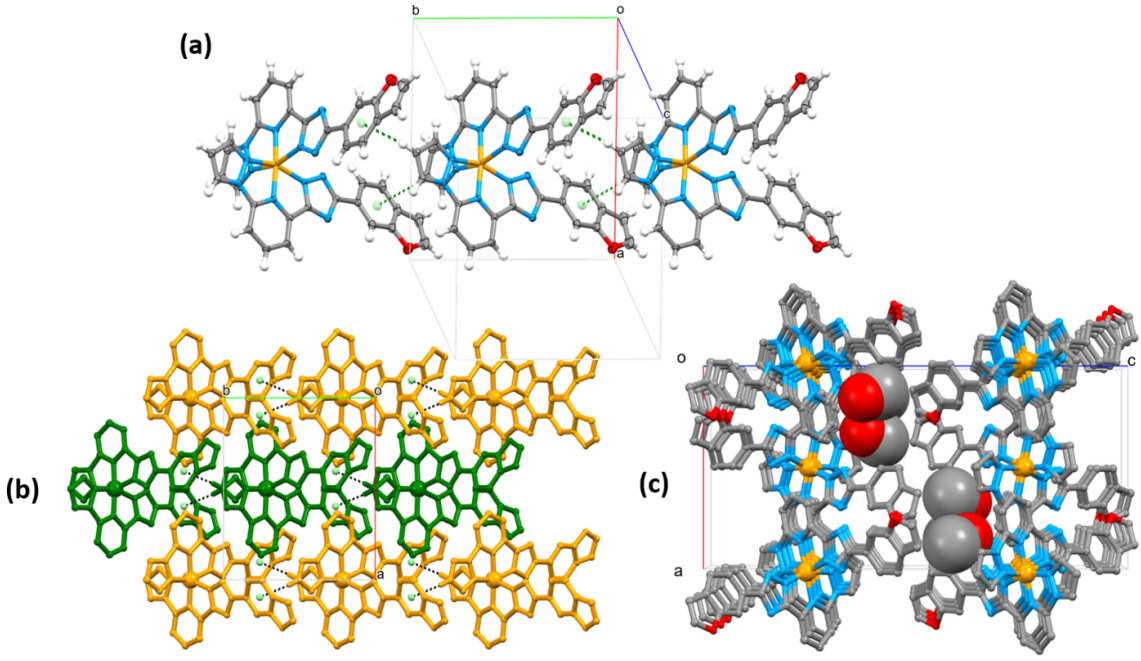

Figure 2
(*a*) A fragment of supramolecular column formed by stacking of molecules along the *b* axis; (*b*) Supramolecular layers formed by stacking of the supramolecular columns in the *ab* plane (for a better representation, each column has a different colour). Hydrogen atoms, except those in pz-groups participating in C–H···*Cg*(π) interactions, are omitted for clarity; (*c*) Stacking of the layers along the *b* axis direction with the methanol molecules in the voids. Hydrogen atoms are omitted for clarity.

1.957 (2) Å and the volume of the [FeN_6] coordination polyhedron of 9.64 Å^3 are small and afor the low-spin state of the central ion (Gütlich & Goodwin, 2004). The average trigonal distortion parameters $\Sigma = \Sigma_1^{12}(|90 - \phi_i|)$, where ϕ_i is the angle N—Fe—N′, and $\Theta = \Sigma_1^{24}(|60 - \theta_i|)$, where θ_i is the angle generated by superposition of two opposite faces of an octahedron, are 90.9 and 315.2°, respectively. The calculated continuous shape measure [CShM(O_h)] value relative to the ideal octahedral symmetry is 2.300 (Kershaw Cook *et al.*, 2015). The values indicate a pseudo-octahedral coordination environment [for an ideal octahedron $\Sigma = \Theta =$ CShM(O_h) = 0].

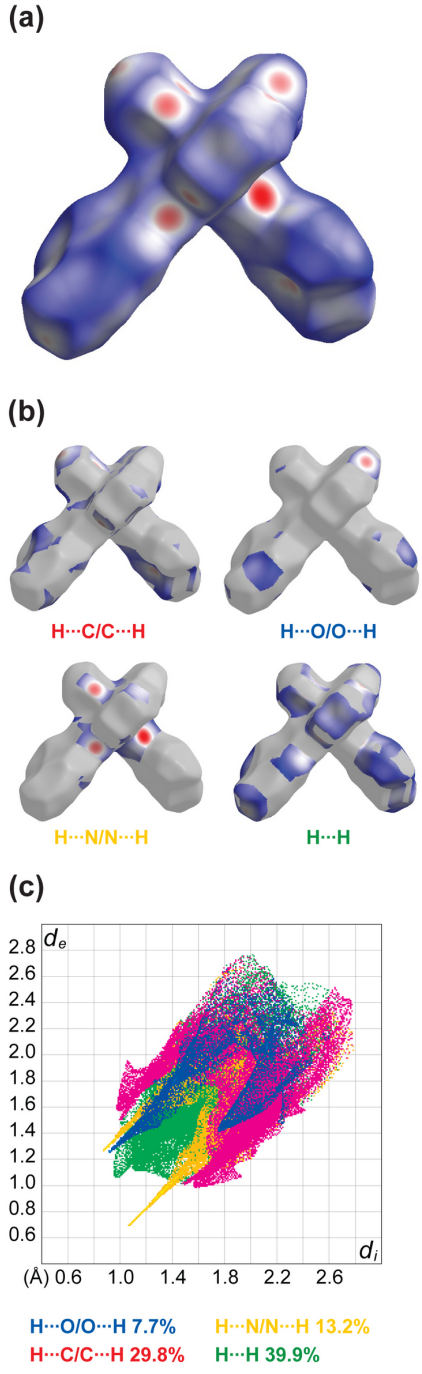

Figure 3
(*a*) A projection of d_{norm} mapped on the Hirshfeld surface identifying contact points or areas for intermolecular interactions on the molecule; (*b*) decomposition of the projection d_{norm} into the specific intermolecular interactions; (*c*) decomposition of the two-dimensional fingerprint plot into specific interactions.

3. Supramolecular features

In the crystal, the molecules interlock by inserting the narrower end of one into the wider end of another, and interact through weak C—H(pz)···π(ph) intermolecular contacts between the pyrazole and phenyl groups [the H2/C2···*Cg*(ph) distance is 2.550 (2)/3.489 (2) Å]. The formed supramolecular chains extend along the *b*-axis direction with a stacking periodicity of 10.5670 (1) Å (Fig. 2). Weak intermolecular C—H(pz, py)···N/C(pz, trz) interactions, ranging from 3.189 (2) to 3.695 (2) Å (Table 1), connect neighbouring chains into layers propagating in the *ab* plane. The voids between the layers are occupied by methanol molecules, which also participate in the bonding within separate layers. The methanol molecules form a strong O—H···N5 hydrogen bond with the deprotonated trz groups and weak C—H···O hydrogen bonds with the pz and py groups of the ligand. A complete list of selected intermolecular interactions is provided in Table 1.

Hirshfeld surface analysis was conducted for the complex to gain a deeper understanding of the interactions. These interactions are visualized as red (d_{norm}< vdW radii), white (d_{norm}= vdW radii), and blue (d_{norm}> vdW radii) spots on the d_{norm} surface for the compound along with fingerprint plots mapped with d_{norm} (where $d_{norm} = d_i + d_e$) and decomposed to the separate contributions (Fig. 3*a*–*c*). At 39.9%, the largest contribution to the overall crystal packing is from H···H interactions, which are located in the middle region of the fingerprint plot. H···C contacts contribute 29.8%, and H···O 7.7%, resulting in pairs of characteristic wings. The H···N contacts, represented by a pair of sharp spikes in the fingerprint plot, make a 13.2% contribution to the surface.

The energy framework (Spackman *et al.*, 2021), was calculated based on the wave function at the B3LYP/6-31G(d,p) theory level. This framework includes components such as electrostatic (E_{ele}), polarization (E_{pol}), repulsion (E_{rep}), and dispersion (E_{dis}) interactions. The latter dominate the contributions, underscoring their primary role for neutral molecules in the crystal structure. The total energy diagram (E_{tot}) overlaid with a fragment of the crystal structure is built using cylindrical bonds between centroids of molecules, where the radii are proportional to the relative interaction strengths (Fig. 4*a*–*c*). The overall topology of the energy framework mirrors the interaction patterns both within and between layers, as outlined earlier. Quantitatively, the E_{tot} for intrachain interactions is −50.1 kJ mol^{-1}, while interchain interactions reach values as low as −81.8 kJ mol^{-1}. Interlayer interactions, in contrast, have an energy as low as −12.2 kJ mol^{-1}. The figure also shows colour-coding of the interactions around a central reference molecule, along with a table of the individual contributions to E_{tot}.

Table 2
Computed distortion indices (Å, °) for the title compound and for similar complexes reported in the literature..

CSD Refcode	azol 1/azol 2	<Fe—N>	Σ	Θ	CShM(O_h)
Title compound	1,2,4-triazole/pyrazole	1.957	90.9	315.2	2.300
BEJQOA	1,2,4-triazole/pyrazole	1.946	87.5	308.9	2.163
ABUFOV	benzimidazole/benzimidazole	1.937	80.1	262.7	1.753
BOWRIR	tetrazole/pyrazole	1.934	89.7	287.4	2.043
XODCEB	benzimidazole/pyrazole	1.950	87.5	276.6	1.925

4. Database survey

A search of the Cambridge Structural Database (CSD, Version 5.42, last update April 2025; Groom *et al.*, 2016) reveals several low-spin neutral Fe^{II} complexes based on asymmetric bisazolpyridines. The selected representative compound for different pairs of azol-azol substituents are ABUFOV (Rajnák *et al.*, 2017), BEJQOA (Seredyuk *et al.*, 2022), BOWRIR (Senthil Kumar *et al.*, 2020) and XODCEB (Shiga *et al.*, 2019). Table 2 collates some key structural parameters of the complexes. Compared to the title compound, the surveyed complexes generally do not bear voluminous substituents and exhibit lower coordination sphere distortion parameters, suggesting that the bulky benzofuran group, rigidly linked to the donor groups in the present ligand, likely induces greater deviation from an ideal octahedral geometry. This observation underscores the significant influence of peripheral substituents on the structural properties of such complexes.

5. Synthesis and crystallization

The synthesis of the title compound followed the protocol reported for a similar complex (Seredyuk *et al.*, 2022). It was produced by a layering technique in a standard test tube. The layering sequence was as follows: the bottom layer contained a solution of $[Fe(L_2)](BF_4)_2$ prepared by dissolving *L* = 3-(benzofuran-6-yl)-5-[6-(1*H*-pyrazol-1-yl)pyridin-2-yl]-4*H*-1,2,4-triazol (100 mg, 0.304 mmol) and $Fe(BF_4)_2{\cdot}6H_2O$ (51 mg, 0.152 mmol) in boiling acetone, to which chloroform (5 ml) was then added. The middle layer was a methanol–chloroform

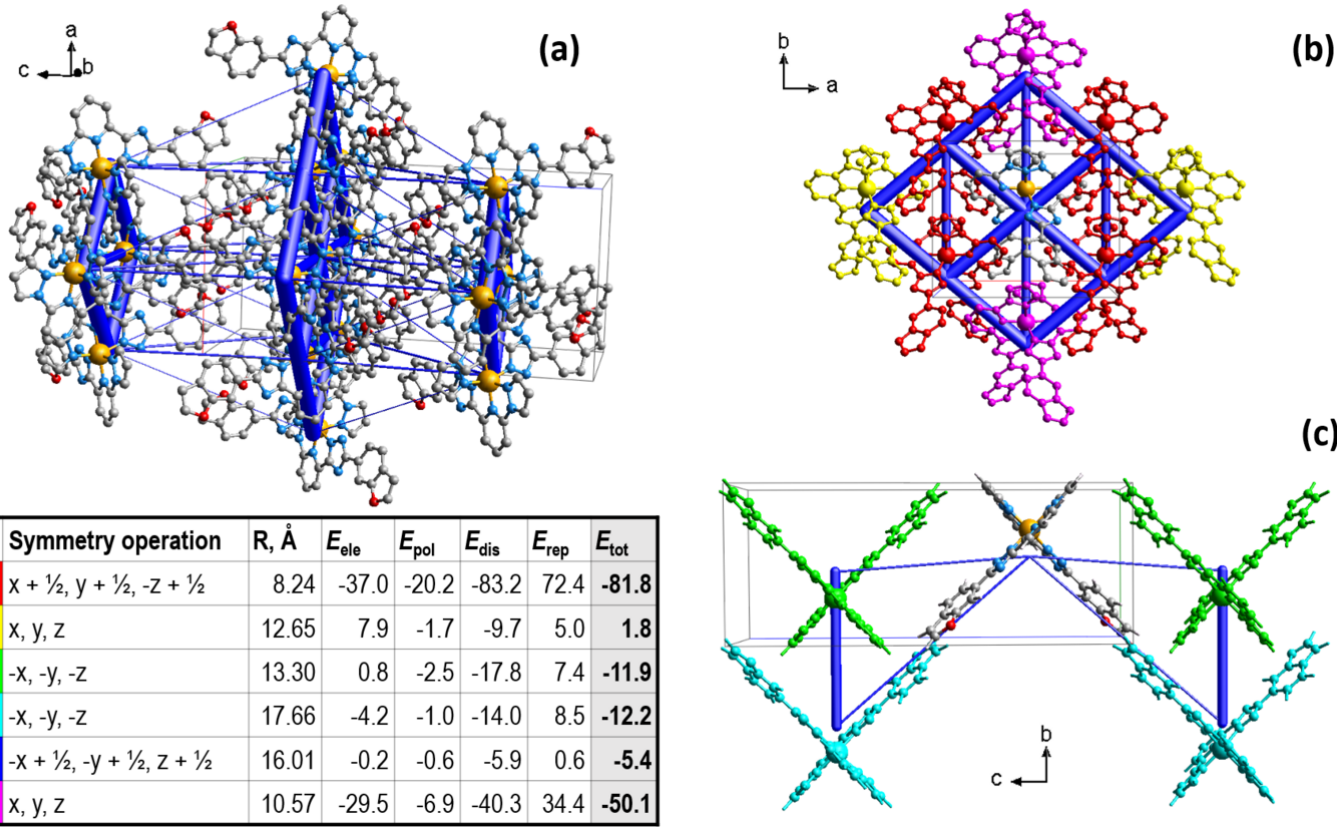

	Symmetry operation	R, Å	E_{ele}	E_{pol}	E_{dis}	E_{rep}	E_{tot}
	x + ½, y + ½, -z + ½	8.24	-37.0	-20.2	-83.2	72.4	**-81.8**
	x, y, z	12.65	7.9	-1.7	-9.7	5.0	**1.8**
	-x, -y, -z	13.30	0.8	-2.5	-17.8	7.4	**-11.9**
	-x, -y, -z	17.66	-4.2	-1.0	-14.0	8.5	**-12.2**
	-x + ½, -y + ½, z + ½	16.01	-0.2	-0.6	-5.9	0.6	**-5.4**
	x, y, z	10.57	-29.5	-6.9	-40.3	34.4	**-50.1**

Figure 4
(*a*) The calculated energy frameworks, showing the total energy diagrams (E_{tot}); (*b*) decomposition of the energy framework into the part corresponding to the intralayer interactions and (*c*) interlayer interactions. In the table, the corresponding colour-coded energy values E_{tot} are provided, including their E_{ele}, E_{pol}, E_{dis}, and E_{rep} components. Tube size is set at 100 scale.

mixture (1:10; 10 ml), which was covered by a layer of methanol (10 ml), to which 100 µl of NEt_3 was added dropwise. The tube was sealed, and dark-red plate-like single crystals appeared after 3–4 weeks (yield *ca*. 80%). Elemental analysis calculated for $C_{38}H_{30}FeN_{12}O_4$: C, 58.92; H, 3.90; N, 21.70. Found: C, 59.14; H, 3.97; N, 22.05.

6. Refinement

Crystal data, data collection and structure refinement details are summarized in Table 3. The hydrogen atom H2*A* was refined freely, other H atoms were refined as riding [C—H = 0.95–0.98 Å with U_{iso}(H) = 1.2–1.5U_{eq}(C)].

Acknowledgements

The authors are grateful to the FAIRE programme provided by the Cambridge Crystallographic Data Centre (CCDC) for the opportunity to use the Cambridge Structural Database (CSD) and associated software. Author contributions are as follows: conceptualization, MS; methodology, KZ; formal analysis, IOF; synthesis, IT; single-crystal measurements, S*S*; writing (original draft), IT and MS; writing (review and editing), KZ and VMA; visualization and calculations, OVO; funding acquisition, MS and KZ.

Funding information

Funding for this research was provided by: Ministry of Education and Science of Ukraine (grant for the perspective development of the scientific direction "Mathematical sciences and natural sciences" at the Taras Shevchenko National University of Kyiv).

Table 3
Experimental details.

Crystal data	
Chemical formula	$[Fe(C_{18}H_{11}N_6O)_2]\cdot 2CH_4O$
M_r	774.59
Crystal system, space group	Orthorhombic, *Pbcn*
Temperature (K)	100
a, *b*, *c* (Å)	12.64747 (16), 10.56703 (12), 26.4991 (4)
V (Å^3)	3541.51 (8)
Z	4
Radiation type	Cu *Kα*
μ (mm^{-1})	3.92
Crystal size (mm)	0.2 × 0.10 × 0.02
Data collection	
Diffractometer	Rigaku R-AXIS Spider
Absorption correction	Multi-scan (*CrysAlis PRO*; Rigaku OD, 2024)
T_{min}, T_{max}	0.534, 1.000
No. of measured, independent and observed [$I > 2\sigma(I)$] reflections	14149, 3464, 3112
R_{int}	0.035
(sin $\theta/\lambda)_{max}$ (Å^{-1})	0.632
Refinement	
$R[F^2 > 2\sigma(F^2)]$, $wR(F^2)$, *S*	0.037, 0.097, 1.05
No. of reflections	3464
No. of parameters	267
H-atom treatment	H atoms treated by a mixture of independent and constrained refinement
$\Delta\rho_{max}$, $\Delta\rho_{min}$ (e Å^{-3})	0.38, −0.30

Computer programs: *CrysAlis PRO* (Rigaku OD, 2024), *OLEX2.solve* 1.5 (Bourhis *et al.*, 2015), *SHELXL2018/3* (Sheldrick, 2015) and *OLEX2* (Dolomanov *et al.*, 2009).

References

Bonhommeau, S., Lacroix, P. G., Talaga, D., Bousseksou, A., Seredyuk, M., Fritsky, I. O. & Rodriguez, V. (2012). *J. Phys. Chem. C* **116**, 11251–11255.

Bourhis, L. J., Dolomanov, O. V., Gildea, R. J., Howard, J. A. K. & Puschmann, H. (2015). *Acta Cryst.* A**71**, 59–75.

Dolomanov, O. V., Bourhis, L. J., Gildea, R. J., Howard, J. A. K. & Puschmann, H. (2009). *J. Appl. Cryst.* **42**, 339–341.

Fares, M., Wu, X., Ramesh, D., Lewis, W., Keller, P. A., Howe, E. N. W., Pérez–Tomás, R. & Gale, P. A. (2020). *Angew. Chem. Int. Ed.* **59**, 17614–17621.

Groom, C. R., Bruno, I. J., Lightfoot, M. P. & Ward, S. C. (2016). *Acta Cryst.* B**72**, 171–179.

Gütlich, P. & Goodwin, H. A. (2004). *Top. Curr. Chem.* **233**, 1–47.

Halcrow, M. A. (2024). *Dalton Trans.* **53**, 13694–13708.

Kershaw Cook, L. J., Mohammed, R., Sherborne, G., Roberts, T. D., Alvarez, S. & Halcrow, M. A. (2015). *Coord. Chem. Rev.* **289–290**, 2–12.

Piñeiro-López, L., Valverde-Muñoz, F. J., Seredyuk, M., Bartual-Murgui, C., Muñoz, M. C. & Real, J. A. (2018). *Eur. J. Inorg. Chem.* pp. 289–296.

Rajnák, C., Titiš, J., Fuhr, O., Ruben, M. & Boča, R. (2017). *Polyhedron* **123**, 122–131.

Rigaku OD (2024). *CrysAlis PRO*. Rigaku Oxford Diffraction, Yarnton, England.

Senthil Kumar, K., Vela, S., Heinrich, B., Suryadevara, N., Karmazin, L., Bailly, C. & Ruben, M. (2020). *Dalton Trans.* **49**, 1022–1031.

Seredyuk, M., Gaspar, A. B., Kusz, J., Bednarek, G. & Gütlich, P. (2007). *J. Appl. Cryst.* **40**, 1135–1145.

Seredyuk, M., Znovjyak, K., Valverde-Muñoz, F. J., da Silva, I., Muñoz, M. C., Moroz, Y. S. & Real, J. A. (2022). *J. Am. Chem. Soc.* **144**, 14297–14309.

Sheldrick, G. M. (2015). *Acta Cryst.* C**71**, 3–8.

Shiga, T., Saiki, R., Akiyama, L., Kumai, R., Natke, D., Renz, F., Cameron, J. M., Newton, G. N. & Oshio, H. (2019). *Angew. Chem. Int. Ed.* **58**, 5658–5662.

Spackman, P. R., Turner, M. J., McKinnon, J. J., Wolff, S. K., Grimwood, D. J., Jayatilaka, D. & Spackman, M. A. (2021). *J. Appl. Cryst.* **54**, 1006–1011.

Wei, S. Y., Wang, J. L., Zhang, C. S., Xu, X.-T., Zhang, X. X., Wang, J. X. & Xing, Y.-H. (2015). *ChemPlusChem* **80**, 549-558.

supporting information

Acta Cryst. (2025). E**81**, 991-995 [https://doi.org/10.1107/S2056989025008655]

Crystal structure, Hirshfeld surface and energy framework analysis of bis-{3-(benzofuran-6-yl)-5-[6-(1*H*-pyrazol-1-yl)pyridin-2-yl]-1*H*-1,2,4-triazol-1-ido}iron(II) methanol disolvate

Illia Terpeliuk, Kateryna Znovjyak, Sergiu Shova, Olexandr V. Oksiuta, Vladimir M. Amirkhanov, Igor O. Fritsky and Maksym Seredyuk

Computing details

Bis{3-(benzofuran-6-yl)-5-[6-(1*H*-pyrazol-1-yl)pyridin-2-yl]-1*H*-1,2,4-triazol-1-ido}iron(II) methanol disolvate

Crystal data

$[Fe(C_{18}H_{11}N_6O)_2]\cdot 2CH_4O$
$M_r = 774.59$
Orthorhombic, *Pbcn*
$a = 12.64747\ (16)$ Å
$b = 10.56703\ (12)$ Å
$c = 26.4991\ (4)$ Å
$V = 3541.51\ (8)$ Å^3
$Z = 4$
$F(000) = 1600$
$D_x = 1.453$ Mg m^{-3}
Cu $K\alpha$ radiation, $\lambda = 1.54184$ Å
Cell parameters from 1992 reflections
$\theta = 2.6–21.9°$
$\mu = 3.92$ mm^{-1}
$T = 100$ K
Plate, clear dark red
0.2 × 0.1 × 0.02 mm

Data collection

Rigaku R-AXIS Spider diffractometer
Radiation source: sealed X-ray tube
Graphite monochromator
ω scans
Absorption correction: multi-scan (CrysAlisPro; Rigaku OD, 2024)
$T_{min} = 0.534$, $T_{max} = 1.000$
14149 measured reflections
3464 independent reflections
3112 reflections with $I > 2\sigma(I)$
$R_{int} = 0.035$
$\theta_{max} = 77.0°$, $\theta_{min} = 3.3°$
$h = -14\rightarrow15$
$k = -10\rightarrow12$
$l = -32\rightarrow31$

Refinement

Refinement on F^2
Least-squares matrix: full
$R[F^2 > 2\sigma(F^2)] = 0.037$
$wR(F^2) = 0.097$
$S = 1.05$
3464 reflections
267 parameters
0 restraints
Primary atom site location: iterative
Hydrogen site location: mixed
H atoms treated by a mixture of independent and constrained refinement
$w = 1/[\sigma^2(F_o^2) + (0.0512P)^2 + 1.8481P]$ where $P = (F_o^2 + 2F_c^2)/3$
$(\Delta/\sigma)_{max} = 0.001$
$\Delta\rho_{max} = 0.38$ e Å^{-3}
$\Delta\rho_{min} = -0.30$ e Å^{-3}

Special details

Geometry. All esds (except the esd in the dihedral angle between two l.s. planes) are estimated using the full covariance matrix. The cell esds are taken into account individually in the estimation of esds in distances, angles and torsion angles; correlations between esds in cell parameters are only used when they are defined by crystal symmetry. An approximate (isotropic) treatment of cell esds is used for estimating esds involving l.s. planes.

Fractional atomic coordinates and isotropic or equivalent isotropic displacement parameters (Å²)

	x	*y*	*z*	U_{iso}*/U_{eq}
Fe1	0.500000	0.71753 (3)	0.250000	0.01699 (12)
N2	0.60321 (11)	0.88309 (13)	0.18316 (5)	0.0211 (3)
N5	0.51474 (11)	0.50739 (14)	0.33332 (6)	0.0212 (3)
N1	0.50229 (10)	0.84881 (14)	0.19681 (6)	0.0201 (3)
N6	0.69158 (11)	0.47812 (14)	0.32708 (6)	0.0248 (3)
O2	0.33165 (11)	0.58628 (13)	0.37969 (6)	0.0337 (3)
H2A	0.388 (2)	0.560 (3)	0.3652 (11)	0.051*
C10	0.60031 (14)	0.44450 (16)	0.34999 (7)	0.0234 (4)
N4	0.55298 (11)	0.58772 (13)	0.29740 (5)	0.0200 (3)
O1	0.76510 (15)	0.11184 (16)	0.45227 (8)	0.0592 (5)
N3	0.64849 (12)	0.72535 (13)	0.23605 (6)	0.0192 (3)
C3	0.60208 (15)	0.97836 (16)	0.14857 (7)	0.0252 (4)
H3	0.661738	1.018159	0.133646	0.028 (5)*
C1	0.43939 (14)	0.92266 (16)	0.16998 (7)	0.0231 (4)
H1	0.364343	0.920088	0.171141	0.018 (5)*
C9	0.65775 (14)	0.56733 (16)	0.29510 (7)	0.0219 (4)
C14	0.59610 (19)	0.17309 (18)	0.46954 (7)	0.0370 (5)
C15	0.50599 (18)	0.2460 (2)	0.46065 (8)	0.0368 (5)
H15	0.444813	0.236306	0.481086	0.034 (6)*
C11	0.59762 (15)	0.34926 (16)	0.39076 (7)	0.0255 (4)
C4	0.68561 (14)	0.81295 (16)	0.20461 (6)	0.0209 (3)
C8	0.71692 (14)	0.64890 (16)	0.26088 (7)	0.0216 (4)
C2	0.49829 (14)	1.00533 (19)	0.13958 (7)	0.0264 (4)
H2	0.471293	1.067668	0.117193	0.035 (6)*
C13	0.68376 (18)	0.19108 (19)	0.43879 (8)	0.0375 (5)
C5	0.79190 (14)	0.83074 (17)	0.19502 (7)	0.0249 (4)
H5	0.816012	0.894204	0.172386	0.035 (6)*
C6	0.86160 (14)	0.75147 (18)	0.22005 (8)	0.0279 (4)
H6	0.935455	0.759817	0.214414	0.028 (5)*
C12	0.68793 (17)	0.27699 (18)	0.39928 (9)	0.0349 (5)
H12	0.749420	0.286094	0.379018	0.035 (6)*
C19	0.3624 (2)	0.6729 (2)	0.41714 (9)	0.0448 (6)
H19A	0.408898	0.737042	0.402292	0.068 (9)*
H19B	0.400247	0.628001	0.443998	0.064 (9)*
H19C	0.299544	0.713942	0.431245	0.071 (10)*
C7	0.82468 (16)	0.65977 (19)	0.25333 (7)	0.0273 (4)
H7	0.872601	0.605658	0.270552	0.029 (5)*
C16	0.50739 (16)	0.33329 (19)	0.42130 (8)	0.0303 (4)
H16	0.446288	0.383066	0.414909	0.031 (6)*

C18	0.6261 (3)	0.0745 (2)	0.50447 (9)	0.0503 (7)
H18	0.583948	0.039318	0.530606	0.066 (9)*
C17	0.7255 (3)	0.0429 (2)	0.49248 (11)	0.0611 (8)
H17	0.764801	−0.020237	0.509770	0.073 (10)*

Atomic displacement parameters (Å²)

	U^{11}	U^{22}	U^{33}	U^{12}	U^{13}	U^{23}
Fe1	0.0157 (2)	0.0172 (2)	0.0181 (2)	0.000	−0.00027 (13)	0.000
N2	0.0203 (7)	0.0218 (7)	0.0213 (7)	0.0000 (6)	0.0010 (6)	0.0024 (6)
N5	0.0224 (7)	0.0200 (7)	0.0212 (7)	−0.0031 (6)	0.0002 (6)	0.0033 (6)
N1	0.0184 (7)	0.0204 (7)	0.0214 (7)	0.0004 (5)	0.0001 (5)	−0.0016 (6)
N6	0.0224 (7)	0.0235 (7)	0.0286 (8)	0.0000 (6)	−0.0013 (6)	0.0059 (6)
O2	0.0288 (7)	0.0369 (7)	0.0354 (8)	−0.0025 (6)	0.0023 (6)	−0.0099 (6)
C10	0.0232 (9)	0.0212 (8)	0.0258 (9)	−0.0024 (7)	−0.0018 (7)	0.0017 (7)
N4	0.0183 (7)	0.0194 (7)	0.0222 (7)	−0.0020 (5)	−0.0005 (5)	0.0014 (6)
O1	0.0574 (11)	0.0473 (9)	0.0729 (12)	0.0010 (8)	−0.0213 (9)	0.0316 (9)
N3	0.0193 (7)	0.0188 (7)	0.0195 (7)	−0.0009 (6)	−0.0001 (6)	0.0003 (5)
C3	0.0303 (9)	0.0224 (8)	0.0229 (9)	0.0005 (7)	0.0014 (7)	0.0047 (7)
C1	0.0230 (9)	0.0233 (8)	0.0230 (8)	0.0041 (7)	−0.0019 (7)	−0.0016 (7)
C9	0.0211 (8)	0.0211 (8)	0.0234 (8)	0.0002 (7)	−0.0014 (7)	0.0028 (7)
C14	0.0639 (15)	0.0252 (9)	0.0218 (9)	−0.0096 (10)	−0.0079 (9)	0.0020 (7)
C15	0.0570 (15)	0.0290 (10)	0.0243 (10)	−0.0052 (9)	0.0058 (9)	0.0013 (8)
C11	0.0314 (10)	0.0217 (8)	0.0234 (9)	−0.0050 (7)	−0.0053 (7)	0.0025 (7)
C4	0.0227 (9)	0.0207 (8)	0.0193 (8)	0.0009 (7)	−0.0007 (7)	0.0009 (6)
C8	0.0210 (8)	0.0209 (8)	0.0230 (8)	0.0014 (7)	−0.0014 (7)	0.0011 (7)
C2	0.0309 (10)	0.0257 (9)	0.0228 (9)	0.0052 (7)	−0.0017 (7)	0.0028 (7)
C13	0.0442 (12)	0.0278 (9)	0.0405 (12)	−0.0042 (9)	−0.0168 (10)	0.0085 (9)
C5	0.0234 (9)	0.0254 (9)	0.0261 (9)	−0.0028 (7)	0.0020 (7)	0.0049 (7)
C6	0.0177 (9)	0.0313 (9)	0.0347 (10)	−0.0005 (8)	0.0014 (7)	0.0048 (8)
C12	0.0333 (11)	0.0309 (10)	0.0405 (12)	−0.0056 (8)	−0.0070 (9)	0.0119 (9)
C19	0.0680 (16)	0.0340 (11)	0.0325 (11)	−0.0132 (11)	0.0105 (11)	−0.0067 (9)
C7	0.0219 (9)	0.0280 (9)	0.0320 (10)	0.0019 (8)	−0.0016 (7)	0.0064 (8)
C16	0.0409 (11)	0.0245 (9)	0.0254 (10)	−0.0021 (8)	0.0026 (8)	0.0021 (8)
C18	0.088 (2)	0.0333 (12)	0.0300 (11)	−0.0088 (13)	−0.0149 (12)	0.0091 (9)
C17	0.084 (2)	0.0421 (13)	0.0570 (16)	−0.0069 (14)	−0.0303 (15)	0.0262 (12)

Geometric parameters (Å, º)

Fe1—N1^{i}	1.9778 (15)	C9—C8	1.458 (2)
Fe1—N1	1.9778 (15)	C14—C15	1.396 (3)
Fe1—N4	1.9770 (14)	C14—C13	1.389 (3)
Fe1—N4^{i}	1.9770 (14)	C14—C18	1.444 (3)
Fe1—N3^{i}	1.9158 (15)	C15—H15	0.9500
Fe1—N3	1.9158 (15)	C15—C16	1.392 (3)
N2—N1	1.375 (2)	C11—C12	1.392 (3)
N2—C3	1.362 (2)	C11—C16	1.409 (3)
N2—C4	1.399 (2)	C4—C5	1.381 (2)

N5—C10	1.345 (2)	C8—C7	1.382 (3)
N5—N4	1.364 (2)	C2—H2	0.9500
N1—C1	1.322 (2)	C13—C12	1.387 (3)
N6—C10	1.352 (2)	C5—H5	0.9500
N6—C9	1.338 (2)	C5—C6	1.385 (3)
O2—H2A	0.85 (3)	C6—H6	0.9500
O2—C19	1.405 (3)	C6—C7	1.391 (3)
C10—C11	1.477 (2)	C12—H12	0.9500
N4—C9	1.344 (2)	C19—H19A	0.9800
O1—C13	1.374 (3)	C19—H19B	0.9800
O1—C17	1.384 (3)	C19—H19C	0.9800
N3—C4	1.331 (2)	C7—H7	0.9500
N3—C8	1.354 (2)	C16—H16	0.9500
C3—H3	0.9500	C18—H18	0.9500
C3—C2	1.364 (3)	C18—C17	1.339 (4)
C1—H1	0.9500	C17—H17	0.9500
C1—C2	1.403 (3)		

N1^{i}—Fe1—N1	90.92 (9)	C14—C15—H15	120.6
N4^{i}—Fe1—N1	92.23 (6)	C16—C15—C14	118.8 (2)
N4—Fe1—N1^{i}	92.23 (6)	C16—C15—H15	120.6
N4—Fe1—N1	159.14 (6)	C12—C11—C10	118.26 (17)
N4^{i}—Fe1—N1^{i}	159.14 (5)	C12—C11—C16	120.36 (18)
N4—Fe1—N4^{i}	92.13 (8)	C16—C11—C10	121.36 (17)
N3^{i}—Fe1—N1^{i}	79.51 (6)	N3—C4—N2	111.09 (15)
N3—Fe1—N1	79.51 (6)	N3—C4—C5	123.59 (16)
N3—Fe1—N1^{i}	96.99 (6)	C5—C4—N2	125.31 (16)
N3^{i}—Fe1—N1	96.98 (6)	N3—C8—C9	109.07 (15)
N3^{i}—Fe1—N4^{i}	79.64 (6)	N3—C8—C7	120.68 (16)
N3^{i}—Fe1—N4	103.86 (6)	C7—C8—C9	130.18 (17)
N3—Fe1—N4	79.64 (6)	C3—C2—C1	106.30 (16)
N3—Fe1—N4^{i}	103.86 (6)	C3—C2—H2	126.8
N3—Fe1—N3^{i}	175.06 (8)	C1—C2—H2	126.8
N1—N2—C4	116.41 (14)	O1—C13—C14	111.21 (19)
C3—N2—N1	111.23 (14)	O1—C13—C12	124.5 (2)
C3—N2—C4	132.29 (15)	C12—C13—C14	124.3 (2)
C10—N5—N4	104.56 (13)	C4—C5—H5	121.7
N2—N1—Fe1	112.69 (10)	C4—C5—C6	116.69 (16)
C1—N1—Fe1	142.05 (12)	C6—C5—H5	121.7
C1—N1—N2	105.17 (14)	C5—C6—H6	119.6
C9—N6—C10	101.33 (14)	C5—C6—C7	120.74 (17)
C19—O2—H2A	107.2 (19)	C7—C6—H6	119.6
N5—C10—N6	114.20 (15)	C11—C12—H12	121.6
N5—C10—C11	123.95 (16)	C13—C12—C11	116.8 (2)
N6—C10—C11	121.82 (16)	C13—C12—H12	121.6
N5—N4—Fe1	139.02 (11)	O2—C19—H19A	109.5
C9—N4—Fe1	114.63 (11)	O2—C19—H19B	109.5
C9—N4—N5	106.35 (13)	O2—C19—H19C	109.5

C13—O1—C17	104.5 (2)	H19A—C19—H19B	109.5
C4—N3—Fe1	119.77 (12)	H19A—C19—H19C	109.5
C4—N3—C8	119.57 (15)	H19B—C19—H19C	109.5
C8—N3—Fe1	120.46 (12)	C8—C7—C6	118.72 (17)
N2—C3—H3	126.8	C8—C7—H7	120.6
N2—C3—C2	106.38 (16)	C6—C7—H7	120.6
C2—C3—H3	126.8	C15—C16—C11	121.32 (19)
N1—C1—H1	124.5	C15—C16—H16	119.3
N1—C1—C2	110.91 (16)	C11—C16—H16	119.3
C2—C1—H1	124.5	C14—C18—H18	127.0
N6—C9—N4	113.56 (15)	C17—C18—C14	105.9 (2)
N6—C9—C8	130.27 (16)	C17—C18—H18	127.0
N4—C9—C8	116.07 (15)	O1—C17—H17	123.5
C15—C14—C18	136.1 (2)	C18—C17—O1	113.0 (2)
C13—C14—C15	118.49 (18)	C18—C17—H17	123.5
C13—C14—C18	105.4 (2)		

Fe1—N1—C1—C2	175.25 (15)	N3—C8—C7—C6	0.5 (3)
Fe1—N4—C9—N6	−179.26 (12)	C3—N2—N1—Fe1	−176.63 (11)
Fe1—N4—C9—C8	3.9 (2)	C3—N2—N1—C1	0.66 (19)
Fe1—N3—C4—N2	−4.37 (19)	C3—N2—C4—N3	−177.97 (17)
Fe1—N3—C4—C5	175.56 (14)	C3—N2—C4—C5	2.1 (3)
Fe1—N3—C8—C9	1.54 (19)	C9—N6—C10—N5	0.5 (2)
Fe1—N3—C8—C7	−175.82 (14)	C9—N6—C10—C11	−177.82 (16)
N2—N1—C1—C2	−0.70 (19)	C9—C8—C7—C6	−176.21 (18)
N2—C3—C2—C1	−0.1 (2)	C14—C15—C16—C11	−0.3 (3)
N2—C4—C5—C6	179.99 (17)	C14—C13—C12—C11	0.3 (3)
N5—C10—C11—C12	170.28 (18)	C14—C18—C17—O1	−0.1 (3)
N5—C10—C11—C16	−11.3 (3)	C15—C14—C13—O1	−179.64 (19)
N5—N4—C9—N6	0.3 (2)	C15—C14—C13—C12	−0.3 (3)
N5—N4—C9—C8	−176.53 (14)	C15—C14—C18—C17	179.4 (3)
N1—N2—C3—C2	−0.4 (2)	C4—N2—N1—Fe1	6.09 (18)
N1—N2—C4—N3	−1.4 (2)	C4—N2—N1—C1	−176.61 (14)
N1—N2—C4—C5	178.66 (17)	C4—N2—C3—C2	176.33 (18)
N1—C1—C2—C3	0.5 (2)	C4—N3—C8—C9	176.42 (15)
N6—C10—C11—C12	−11.6 (3)	C4—N3—C8—C7	−0.9 (3)
N6—C10—C11—C16	166.86 (18)	C4—C5—C6—C7	−0.5 (3)
N6—C9—C8—N3	−179.67 (17)	C8—N3—C4—N2	−179.28 (14)
N6—C9—C8—C7	−2.6 (3)	C8—N3—C4—C5	0.6 (3)
C10—N5—N4—Fe1	179.40 (14)	C13—O1—C17—C18	−0.1 (3)
C10—N5—N4—C9	0.06 (18)	C13—C14—C15—C16	0.3 (3)
C10—N6—C9—N4	−0.5 (2)	C13—C14—C18—C17	0.2 (3)
C10—N6—C9—C8	175.77 (18)	C5—C6—C7—C8	0.2 (3)
C10—C11—C12—C13	178.16 (17)	C12—C11—C16—C15	0.3 (3)
C10—C11—C16—C15	−178.12 (18)	C16—C11—C12—C13	−0.3 (3)
N4—N5—C10—N6	−0.4 (2)	C18—C14—C15—C16	−178.8 (2)
N4—N5—C10—C11	177.92 (16)	C18—C14—C13—O1	−0.3 (2)
N4—C9—C8—N3	−3.5 (2)	C18—C14—C13—C12	179.1 (2)

N4—C9—C8—C7	173.51 (19)	C17—O1—C13—C14	0.2 (3)
O1—C13—C12—C11	179.6 (2)	C17—O1—C13—C12	−179.1 (2)
N3—C4—C5—C6	0.1 (3)		

Symmetry code: (i) −*x*+1, *y*, −*z*+1/2.

Hydrogen-bond geometry (Å, º)

D—H···*A*	*D*—H	H···*A*	*D*···*A*	*D*—H···*A*
O2—H2*A*···N5	0.85 (3)	1.89 (2)	2.750 (2)	178 (3)
C1—H1···N6^{ii}	0.95	2.27	3.189 (2)	163
C3—H3···O2^{iii}	0.95	2.29	3.208 (2)	161
C5—H5···O2^{iii}	0.95	2.46	3.386 (2)	164
C5—H5···N5^{iii}	0.95	1.90	3.463 (2)	129
C7—H7···C1^{iv}	0.95	2.63	3.537 (2)	159
C19—H19*A*···N2^{i}	0.97	2.74	3.491 (2)	133
C19—H19*A*···C3^{i}	0.97	2.89	3.695 (2)	140
C6···C3^{v}	–	–	3.482 (2)	–
C7···C3^{v}	–	–	3.498 (2)	–

Symmetry codes: (i) −*x*+1, *y*, −*z*+1/2; (ii) *x*−1/2, *y*+1/2, −*z*+1/2; (iii) *x*+1/2, *y*+1/2, −*z*+1/2; (iv) *x*+1/2, *y*−1/2, −*z*+1/2; (v) −*x*+3/2, *y*−1/2, *z*.